

## Magnetic structures in Co-Cr films for perpendicular recording

Cock LODDER, Sietze DE HAAN, Matthijs VAN KOOTEN, Hans TE LINTELO and Steffen PORTHUN

MESA Research Institute, University of Twente, P.O.Box 217, 7500 AE Enschede, The Netherlands

Abstract—Recently it has been shown that the areal density of Co-Cr media for perpendicular recording using a single pole head can be in the order of 5-10 Gbit/ inch<sup>2</sup> [1]. In this laboratory demonstration a track pitch of 0.5  $\mu\text{m}$  (50 kTPI) and a bit length of 260 nm (100 kFRPI) was achieved. Using the same recording set-up, in this paper a MFM image is shown using 300 kFRPI linear bit density and a track width of 0.4  $\mu\text{m}$ . With these densities, microstructural features like columnar size, compositional separation of Co and Cr, magnetic coupling and reversal behaviour become more and more important. This paper presents experimental results obtained from Co-Cr thin films by using MFM, study of artificially etched micro-strips and measuring anomalous Hall effect from submicron structures, as well as results obtained from magnetostatic and micromagnetic simulations.

### I. INTRODUCTION

Exponential increase in recording density has resulted in bit dimensions that approach the fundamental structural dimensions (i.e. columnar / crystal size and surface topology) and intrinsic magnetic dimensions ('domains'). Because of the strong relation between the micro-structure and micromagnetic behaviour, the macromagnetic characterisation by VSM and torque measurements are no longer sufficient to understand the micromagnetic behaviour. To bridge the gap between micro- and macroscopic behaviour in the case of Co-Cr thin film media for perpendicular recording, we started a systematic study which consisted of three complementary experimental parts, i.e. a) investigation of the relation between shape and magnetic behaviour in artificially etched 'bits', b) measurement of the switching behaviour of individual magnetic entities in sub-micron Hall-crosses, and c) observation of micro-structure and written bits by AFM and MFM. Results from these mesoscopic measurements serve as input for micromagnetic simulations. In this paper an overview of these subjects will be given by presenting experimental data mainly obtained from Co-Cr sputtered thin films having a strong perpendicular anisotropy based on highly c-axis textured hcp-structure. All samples show a columnar morphology with a columnar diameter of app. 1/7<sup>th</sup> of the film thickness.

Although the presented results are obtained from Co-Cr samples used for perpendicular recording applications they can be also of interest for the nowadays used Co-Cr-X / Cr (X=Ta,Pt etc.) high density longitudinal media, in spite of the absence of a perpendicular demagnetising field in these media. This demagnetising field plays an important role in the magnetisation reversal in Co-Cr media with perpendicular anisotropy. In our opinion it is still not clear how the magnetisation is reversed and what exactly the influence from micro-structure and morphology on the reversal is. The magnetic uncoupling of the columns by the column-boundaries and the compositional separation in the columns itself are playing a key role in the behaviour, but there are not many consistent experimental data available showing what is really happening on the scale of the current bit size dimensions. Although we also do not

have this data available, we have made a start to try to find a more consistent relation between micro-structural properties, macroscopical magnetic measurements, information on mesoscopical scale and micromagnetic simulations. This paper presents some first results.

### II. STUDY OF SHAPE ANISOTROPY BY ARTIFICIALLY ETCHED MICRO-STRIPS

The influence of bit size and shape on magnetic behaviour of perpendicular magnetic media is investigated by artificially etching micro-strips. In this way the demagnetising field is manipulated whereas the intrinsic properties like saturation magnetisation  $M_s$  and crystal anisotropy  $K_1$  are unaffected. Objective is to extract information on the role of demagnetisation in reversal processes and to relate this to magnetic behaviour of written bits. At the same time stray field measurements are performed which are compared to written bits and stray field calculations.

The Co-Cr films were RF sputtered from alloyed targets (Cr content: 19, 21 and 23 at.%) under optimised conditions [2]. Photolithography was performed, using a positive resist (Shipley S1400-31), and ion beam milling ( $V_{\text{acc}} = 500 \text{ V}$ ,  $I_{\text{cath}} = 12.5 \text{ mA}$ , Ar flow = 200 sccm) which caused no annealing effects on the Co-Cr. The patterned Co-Cr exhibits a bit-shaped structure. The strip width and length are in the order of 1 to 5  $\mu\text{m}$  and the period is varied in both x- and y-direction. In fig. 1 a SEM photograph shows a typical example. All samples exhibit a uniaxial anisotropy perpendicular to the substrate which

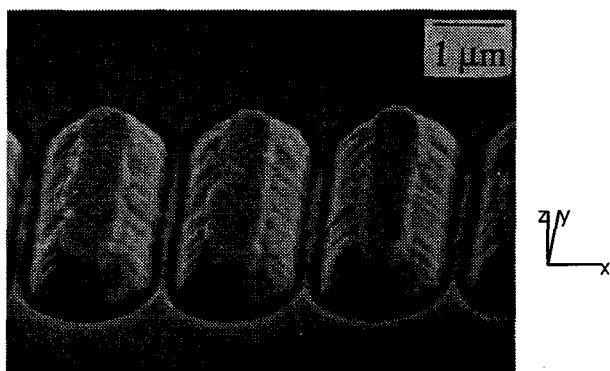


Fig. 1. SEM photograph of patterned Co-Cr micro-strips.

is larger than the (diminished) demagnetisation ( $Q > 1$ ). A more detailed description of the magnetic properties is given in references [3,4].

In order to understand the magnetic behaviour of a ferromagnetic body (or written bit) it is essential to know the field the magnetisation  $M$  experiences inside the ferromagnetic body. This internal field  $H_{int}$  is given for the perpendicular direction (z-axis) by:

$$H_{int} = H_{ext} - N_z M \quad (1)$$

where  $H_{ext}$  is the externally applied field and  $N_z$  is the demagnetisation factor, i.e. the volume average of the demagnetising field. Due to this demagnetisation the hysteresis curve becomes sheared, as is indicated in fig. 2. Here a typical example of the demagnetising influence on the shearing of the perpendicular loop is shown for an as-sputtered sample and a corresponding patterned Co-Cr sample. Both curves show a similar shape, however, the as-sputtered sample exhibits less shearing of the curve ( $N_z = 1$ ). The observed decrease in shearing with  $N_z$  is in qualitative agreement with eq. 1, from which it is concluded that the susceptibility  $\chi$  depends on [5]:

$$\chi = \frac{\partial M}{\partial H} \approx \frac{1}{N_z} \quad (2)$$

We investigated this relation also quantitatively by measuring the demagnetisation factor. This was obtained by comparing torque measurements of patterned samples to their corresponding as-sputtered samples [3] so that the shape anisotropy contribution was isolated from the other anisotropies present in the material. It appeared that eq. 2 is correct in first approximation. Also the increase in remanence and change in stripe-out field could be understood from eq. 1, leading to the conclusion that the magnetic behaviour of the assembly of micro-strips can be well understood from a mean internal field description.

Also time dependent VSM-measurements were performed to provide additional information on the relation between

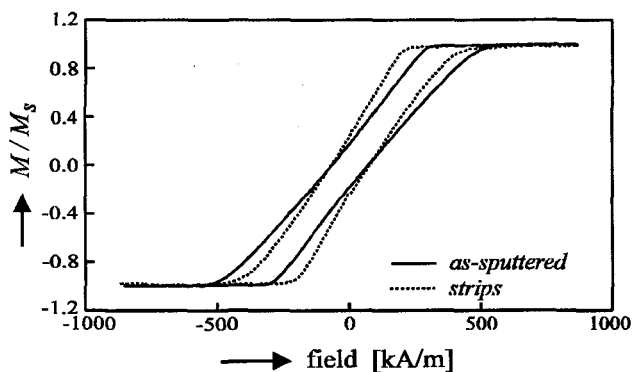


Fig. 2: Perpendicular hysteresis curves for Co-Cr micro-strips (dashed line) and its corresponding reference sample (solid line).

demagnetisation and the reversal process. The time dependence is characterised by the magnetic viscosity parameter  $S$  which is directly associated with the microscopic structure of materials and with the processes responsible for magnetisation [6]. Therefore these macroscopic measurements should result in information on microscopic entities such as the magnetic activation volume, and thus on the influence of demagnetisation on magnetisation reversal.

The magnetic after-effect describes the relaxation of a metastable system towards a more stable state. It has its origin in thermally activated transitions over energy barriers, which is given for a single barrier by the Arrhenius-Néel law. When a dispersion of energy barriers is present in the material, however, the decay in magnetisation is generally described by the logarithmic relation:

$$M(t) = M(0) + S \ln(t) \quad (3)$$

where  $M$  is the perpendicular magnetisation at time  $t$ , or at the start of the measurement ( $t = 0$ ). The coefficient of magnetic viscosity  $S$  exhibits information on the fluctuation field  $H_f$  which represents a fictitious field needed to reverse the thermally activated volumes. For samples where the demagnetisation factor  $N_z$  is not equal to zero the magnetic viscosity is related empirically to this fluctuation field through the equation [7].

$$H_f = \frac{S}{\chi_a^{tot}} (1 - N_z \chi_a^{rev}) \left( \frac{\chi_a^{tot}}{\chi_a^{tot} - \chi_a^{rev}} \right) \quad (4)$$

where  $\chi_a^{tot}$  denotes the total volume susceptibility measured as the change in intensity of magnetisation per unit change of applied field, and  $\chi_a^{rev}$  denotes the reversible component. From eq. 4 it can be seen that for materials exhibiting a negligible reversible component of the susceptibility, the last two terms equal one. When  $H_f$  is an intrinsic material property this implies that the magnetic viscosity exhibits a linear relation with the total susceptibility. Consequently  $S$  will increase with decreasing  $N_z$

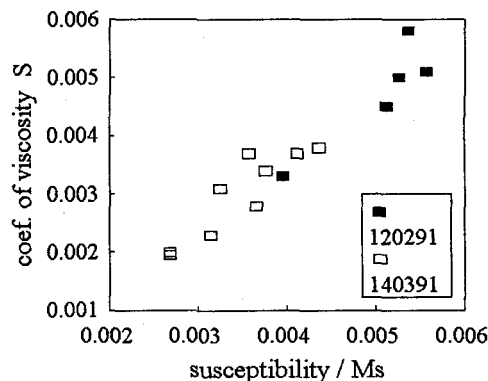


Fig. 3: The coefficient of magnetic viscosity as a function of the total susceptibility, measured at zero applied field.

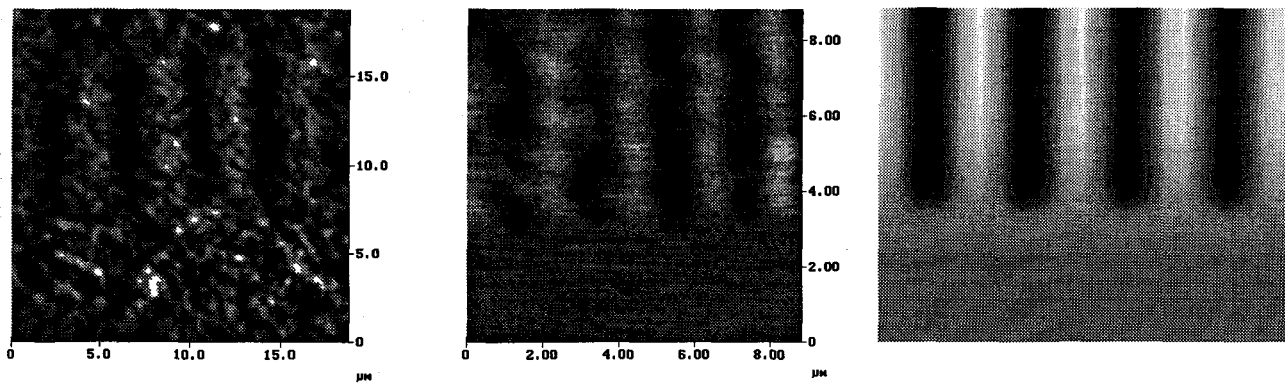


Fig. 4. Magnetic stray field gradient measured by MFM above a written bit track (left), above micro-strips (center) and above magnetostatically simulated micro-strips (right).

(see fig. 2). This results in a larger time dependence for patterned perpendicular media in comparison to their as-sputtered equivalents. This is visualised in fig. 3 where two series of hard magnetic Co-Cr films (120291 and 140391) are patterned into different shapes and therefore  $N_z$ . Their susceptibility and magnetic viscosity is measured and is shown to exhibit a linear relationship with  $N_z$ .

Besides the magnetic behaviour inside the micro-strip also the magnetic stray fields outside the strips was measured. This serves the purpose of investigating the stray field for well-characterised micro-shapes as a function of varying magnetic properties. The objective was to relate the results of these well-defined structures to written bits and similar shapes. The stray field was revealed by Lorentz microscopy and MFM. Because the results of the former are published elsewhere [8] only the MFM results will be shown.

In fig. 4 a typical example of the stray field above micro-strips ( $1\mu\text{m}$  width and  $10\mu\text{m}$  long) and written bits (bit wave length is  $4\mu\text{m}$ ) is shown. Except for a remanent domain structure present in the written bit sample, the stray fields of both figures show a clear resemblance. This resemblance is to be expected from magneto-static considerations because written bits are equivalent to micro-strips where the gaps in between the strips are filled with a reversed magnetisation (see fig. 1). Whereas the intrinsic behaviour of the micro-strips could be understood from mean field theory we also calculated the stray field by considering the strips as being uniformly perpendicular magnetised. In the right figure of fig. 4 the simulated equivalent is shown. This simulation also confirms that in a first approximation the micro-strips (and written bits) can be understood from a mean field theory.

### III. STUDY OF REVERSAL BY ANOMALOUS HALL MEASUREMENTS AND MICRO-MAGNETIC SIMULATION

Anomalous Hall effect (AHE) measurements are applied on very small Co-Cr Hall-samples. With suitable e-beam lithography and ion-beam etching, the measurement area can be made as small as  $300\text{ nm}^2$  [9]. By recording AHE-

loops of these samples, the reversal can be clarified up to a great extent. For this purpose, we used the step size distribution in the measured hysteresis loop [10]. To interpret the measured hysteresis loops, simulations are necessary to check whether intuitive models are correct or need extension. Micromagnetic simulations are believed to be most suitable for this task, because they start with basic principles (exchange, magnetisation, anisotropy and morphology) and yield hysteresis loops and magnetisation patterns. The morphology, the texture and the composition are incorporated into the model by varying the exchange, the magnetisation and the anisotropy locally.

A Co-Cr sample with a Cr-content of 23 at.% is sputtered on a Si-substrate covered with a thin layer of  $\text{SiO}_2$ . The unetched sample has an  $M_s$  of  $321\text{ kA/m}$  and a perpendicular coercivity  $H_c$  of  $93\text{ kA/m}$ . The film thickness is  $200\text{ nm}$  and the average column size at the surface is  $60\text{ nm}$ . The samples are etched to a Hall cross geometry with a central area as small as  $300\text{ nm}^2$  [11]. The measurement area contains approximately 40 columns. The largest part of the Hall voltage comes from the central area of the sample of  $300\text{ nm}^2$  [12].

In the anomalous Hall effect measurement set-up, a current is sent through the sample, and the voltage perpendicular to the current, the Hall voltage, is measured in an externally applied field. The hysteresis loop of an etched sample together with an unetched sample is shown in fig. 6 [9].

The influence of the small Hall cross geometry results in a less shearing of the Hall loop and to an increase of the coercivity by 16 % [9]. Less shearing is caused by a decrease of the demagnetisation factor  $N_z$  with the Hall cross size as has been shown for the microstrips in fig. 2. The increase in coercivity is probably caused by more pinning points on the edges of the cross which makes reversal by domain wall movement more difficult.

From MFM-images of the same material it has been shown that the domainsize in the remanent state is around  $150\text{ nm}$  which indicates that app. 4 domains are present in the Hall cross in the remanent state.

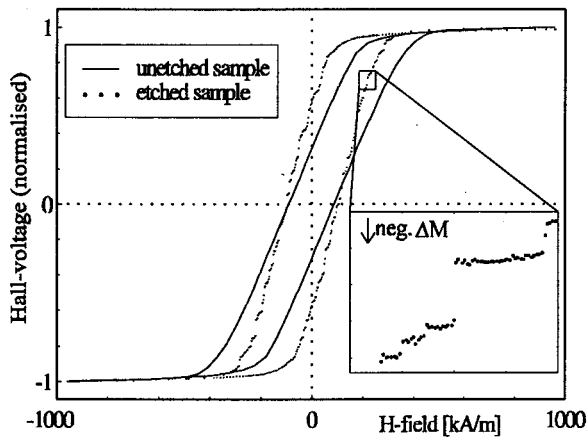


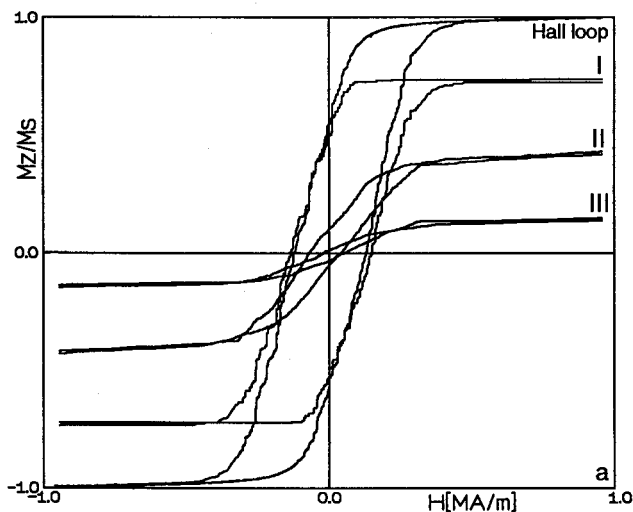
Fig. 5. The normalised AHE hysteresis curves of the unetched (solid curve) and of the etched sample with a Hall cross of  $0.3 \times 0.3 \mu\text{m}$  (dots), with in the inset an enlargement of the steps observed in the etched samples.

The loop in fig. 5 (solid line) shows many more large discrete magnetisation changes (steps) as there are columns and a more or less continuous magnetisation change between the steps. Further, changes with a negative  $\Delta M$  (see the inset of fig. 5) can be seen. Only a few large steps corresponding to the switching of one column are found, but most steps are smaller than 2 % of  $M_s$ , corresponding to less than half a column. The Johnson noise of the sample is the main source of noise and is estimated to correspond with  $0.001 M_s$  in the Hall-loop.

The measured hysteresis loops are decomposed as follows: The changes in magnetisation  $\Delta M$  after each field step are categorised into five different classes:

- I.  $\Delta M > 0.003 M_s$  (equiv. to volumes  $> (30 \text{ nm})^3$ ),
- II.  $0.003 M_s > \Delta M > 0.001 M_s$ ,
- III.  $0.001 M_s > \Delta M > 0$ ,
- IV.  $0 > \Delta M > -0.001 M_s$  and
- V.  $-0.001 M_s > \Delta M$ .

The steps of the different classes are put together to a



Stepsize-distinguished Partial Hysteresis loops (SPH). The superposition of the SPH's from class I, II and III yields a loop with a 'saturation magnetisation' of  $1.3 M_s$ . The Hall loop together with the SPH's are shown in fig. 6. The shapes of the SPH's are very different.

Loop I in fig. 6a, consisting of  $\Delta M$ 's from class I, is an almost ideal hysteresis loop of a particulate medium with perpendicular anisotropy and a sharp Switching Field Distribution. The loop shows the usual shearing due to demagnetisation, a sharp onset of magnetisation reversal, and only a small 'tail', a decrease of the slope at the end of magnetisation reversal. The coercivity is 10 % higher than the coercivity of the original hysteresis loop. Loop II, consisting of  $\Delta M$ 's from class II, is clearly different. It shows a gradual onset of magnetisation reversal, no tail, and a coercivity which is about half of the film coercivity. The loop consisting of negative changes above the noise-level (V in fig. 6b) has the same properties as loop II, except for the lower saturation value. The loops consisting of magnetisation changes below the noise level (III and IV) show hysteresis and saturation. We tend to attribute this at least partly to magnetisation reversal.

The number of magnetisation changes of class I is 155, much larger than the number of columns in the measurement area. This indicates that the column is not the smallest magnetic unit in this particular Co-Cr film. A micro structure which could explain this is the CP structure [13], where small Co-rich platelets are embedded in a Cr-rich matrix inside the column. The small changes can be explained by reversible rotation of regions with in-plane anisotropy [14], which have no perpendicular anisotropy. The negative  $\Delta M$ 's might indicate the presence of magnetic volumes at the limit of superparamagnetism. According to the step size, their volume could be around  $(20 \text{ nm})^3$ . When using the Néel-Arrhenius law for time decay in particle assemblies  $1/t = 10^{-9} \exp(K_1 V/kT)$  [15] the estimated superparamagnetic limit of Co-Cr is  $(8 \text{ nm})^3$  when using a

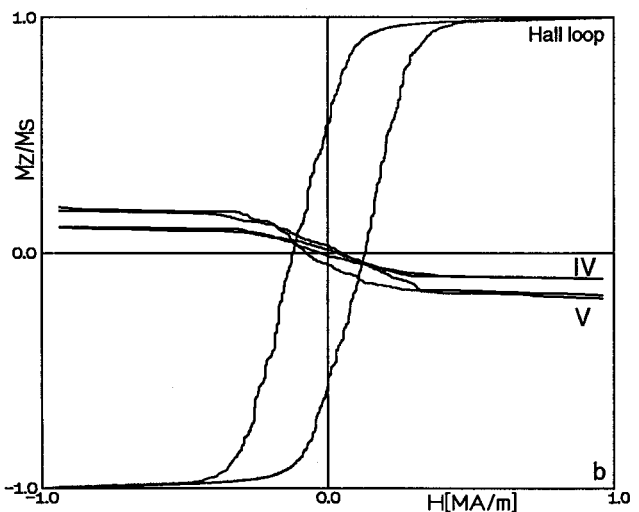


Fig. 6. The original Hall loop and the various Stepsize-distinguished Partial Hysteresis loops (SPH's).

relaxation time  $t$  of 100 s and an anisotropy constant  $K_1$  of  $1.6 \cdot 10^5 \text{ J/m}^3$ . For particulate media, it is also observed that the mentioned formula does predict the so called activation volume, which is much smaller than the particle volume [16]. The magnitude of the SPH of class V can be an indication for the volume fraction of magnetic units at the superparamagnetic limit. With a micromagnetic model, the influence of some microstructural parameters on the observed magnetic behaviour are investigated.

The used micromagnetic model [17], consists of particles (Co-Cr columns) in the shape of cubes of  $(50 \text{ nm})^3$  which are subdivided into cubic elements of  $(5 \text{ nm})^3$  with uniform magnetisation. Exchange between the particles is modelled by assigning an exchange to a few randomly chosen element-pairs which are on the particle boundaries. The initial layer, as present in our Co-Cr, is modelled by assigning an in-plane easy axis to cubes of 8 elements in the bottom two rows of elements in the model. These cubes are exchange coupled to the particle they belong to. This partly overcomes the well-known problem of a too high  $H_c/H_k$  in micromagnetic simulations [18] since it reduces the coercivity by more than 30 %. Further reduction of the coercivity can be obtained by assuming that small regions have a higher  $K_1$  and/or a lower  $M_s$ , such that saturation of the entire film is not saturated below reasonable fields used in a measurement set-up. These regions serve as nucleation centres for magnetisation reversal [19]. Because the Hall-measurements prove that the average magnetic unit size is not equal to the column size, each column is modelled as a Co-poor matrix with 3 Co-rich platelets. The platelets extend throughout the film thickness, the lateral dimensions are  $10 \times 40 \text{ nm}^2$ . Subdivided in this way, the ratio between Co-rich and Co-poor material is app. 1/2.

Typical simulated in-plane and perpendicular hysteresis loops of a 25 particle cluster are shown in fig. 7. The initi-

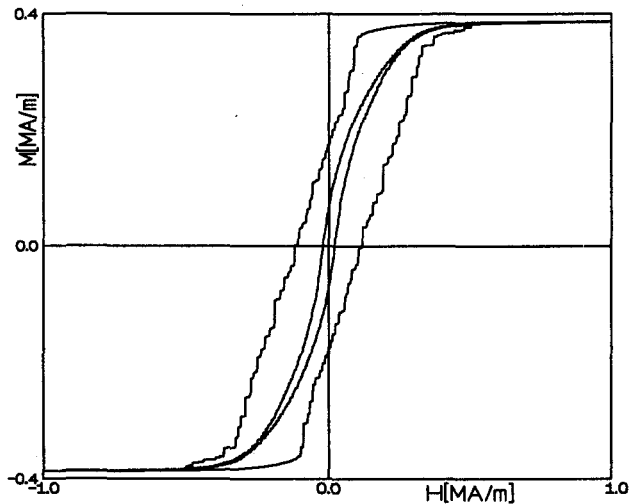


Fig. 7. Simulated in-plane and perpendicular (outer loop) hysteresis loops. See text for parameters.

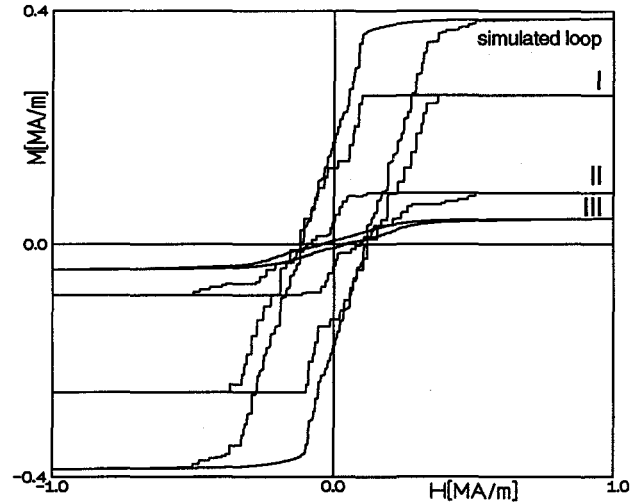


Fig. 8. Decomposition of a simulated hysteresis loop.

al layer volume is 12 %, the hard nucleation centres have a fourfold  $H_k$ , the Co-rich platelets are assumed to have an  $M_s$  of 500 kA/m and a  $K_1$  of 160 kJ/m<sup>3</sup>. For the Co-poor matrix these values are 300 kA/m and 50 kJ/m<sup>3</sup>. The coercivity is 110 kA/m, there is a modest shoulder present which is not seen in highly segregated films, but for the rest there is close resemblance in shape with experimental loops. The stepsizes show that platelets predominantly switch independently.

Decomposition of the perpendicular loop of fig. 7 is shown in fig. 8. The class-thresholds are: I  $\Delta M > 0.03 M_s$ , II  $0.03 M_s > \Delta M > 0.003 M_s$  and III  $0.003 M_s > \Delta M$ . It can be seen that the loop with the larger steps shows the same sharp onset of reversal and the loop with the smaller steps a gradual one, resembling the experimental result well.

#### IV. MAGNETIC FORCE MICROSCOPY

For a more detailed study of the Co-Cr-X layers with perpendicular anisotropy Magnetic Force Microscopy (MFM) studies are carried out. Easy sample preparation and the achievable resolution make this method very suitable.

Our MFM set-up is based on a Michelson type interferometer for cantilever deflection detection [20]. We use magnetic tips made from magnetically coated carbon needles which are grown in an electron beam on the end of a tungsten wire cantilever [21]. This set-up allows to resolve magnetic details smaller than 30 nm. [20]

High density written bits on a Co-Cr-Ta hard disk with a bit length close to or even smaller than the size of the intrinsic domain structure are used for our study. The Co-Cr-Ta layer had a thickness of 70 nm and was grown on a 7  $\mu\text{m}$  thick underlayer of NiFe. The columnar diameter of the Co-Cr-Ta is about 10 nm. By single pole head bit tracks of up to 500 kfrpi (kilo flux reversals per inch) have been written on this disk on tracks of 30  $\mu\text{m}$  and 0.4  $\mu\text{m}$  width. Both disk fabrication and bit writing have been carried out in Tohoku University Sendai, Japan [1,22].

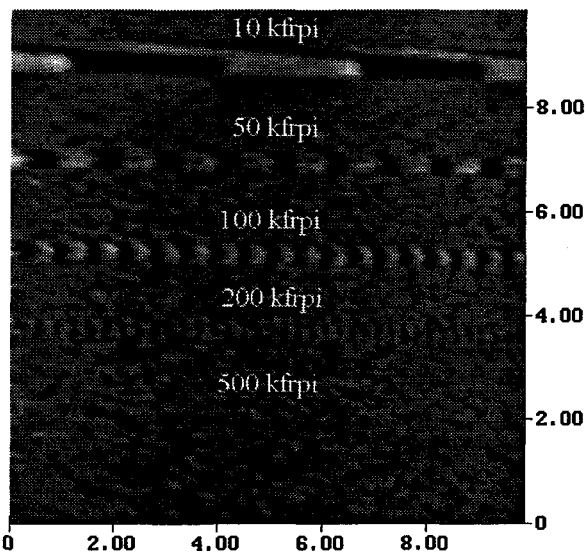


Fig. 9. Overview over a group of  $0.4 \mu\text{m}$  wide tracks.

The size of the intrinsic domains measured next to the bit tracks is about  $150 \text{ nm}$ . For bit densities of about  $200 \text{ kfrpi}$ , the bit length ( $127 \text{ nm}$ ) will become smaller than the intrinsic domain size. Consequently, the bits can not be expected to stay as they have been written. The influence of the magnetic relaxation in the material after the writing head has passed will increase when the bits are made smaller.

Fig. 9 shows an overview over a group of  $0.4 \mu\text{m}$  wide tracks on the disk. The writing densities of the tracks are  $10$ ,  $50$ ,  $100$ ,  $200$  and  $500 \text{ kfrpi}$  from top to bottom. The  $500 \text{ kfrpi}$  track (bit-length  $51 \text{ nm}$ ) is not visible in this image, even with higher magnification and smaller tip-sample distance no difference between this track and the surrounding domain structure could be found.

Fig. 10 gives a zoom in at the  $200 \text{ kfrpi}$  track, measured at

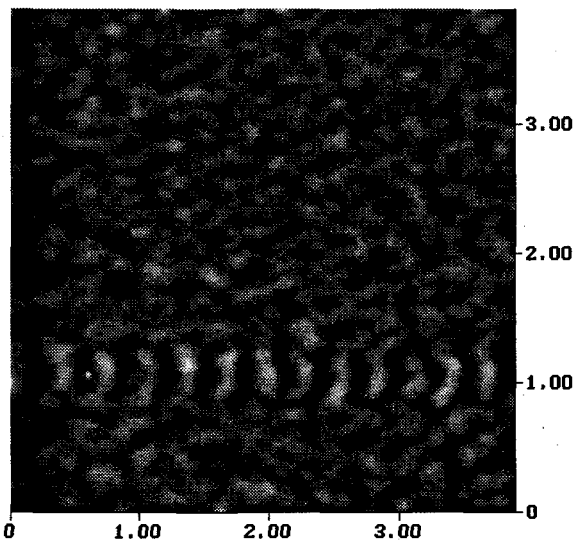


Fig. 10.  $200 \text{ kfrpi}$  bit track on a Co-Cr-Ta disk.

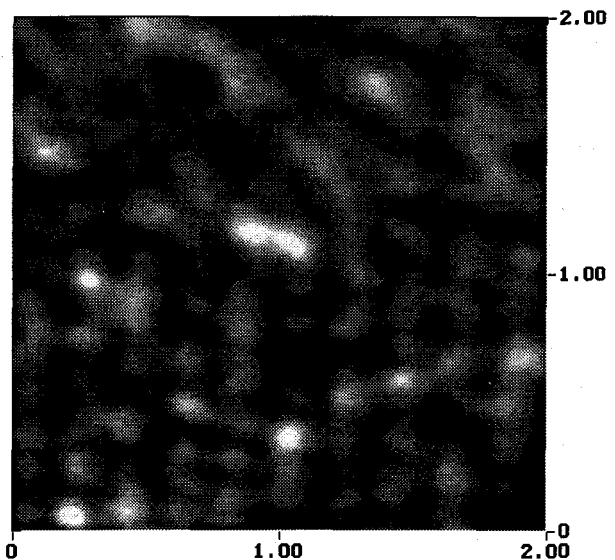


Fig. 11. Side border of a  $30 \mu\text{m}$  wide  $300 \text{ kfrpi}$  bit track.

a smaller tip-sample distance, which clearly shows how the individual bits differ because of the relaxation process after bit writing. The side border of the track is not straight any more because some bit domains are connected to the outside domain pattern. These two effects will certainly contribute to the media noise of this disk when the bits are read back.

Fig. 11 shows the side border of a  $30 \mu\text{m}$  wide  $300 \text{ kfrpi}$  bit track (bit-length  $85 \text{ nm}$ ). Since the image is not as clear as others it will be explained in more detail here. Since the scan is only  $2 \times 2 \mu\text{m}^2$  wide it shows only a small part of the  $30 \mu\text{m}$  wide track. The stripe structure in the lower part of the image represents the bits. It is clearly visible that they are smaller than the intrinsic domains in the upper part of the image. Because of the relaxation processes, which takes place in the decreasing head field after the writing head has passed by, each bit is not a single domain but consists of oppositely magnetised domains perpendicular to the track direction. Since a magnetic read head will integrate over the whole track width the signal is still reproduceable but the noise will increase.

Another interesting aspect is that the side border of the track becomes a smooth transition between off-track domains and written domains. Some written bits continue outside the domain structure.

## V. CONCLUSIONS AND SUMMARY

From the influence of bit size and shape on magnetic behaviour of perpendicular magnetic media it is concluded that for Co-Cr micro-strips with dimensions down to one micron its behaviour can be well-understood from mean field considerations. This means that in a first approximation the influence of magnetic micro-structure can be disregarded for magnetic stray-field interpretation. For

magnetic (bit) shapes in the order of the magnetic micro-structure however an anomalous behaviour is to be expected.

AHE measurements showed that the analysis of hysteresis loops of sub-micron Co-Cr samples on the basis of the measured magnetisation changes yields information on distinguishable magnetic volumes in the sample. The size of the measured discrete magnetisation changes shows that the average magnetic unit in Co-Cr is considerably smaller than one column. We observed five steps of approximately one column, the rest of the steps is smaller. From the presence of negative  $\Delta M$ 's and their distribution along the hysteresis loop we conclude that magnetic units on the limit of superparamagnetism could be present in Co-Cr. Magnetic viscosity measurements and temperature dependent hysteresis measurements will have to give more information about this.

The micromagnetic simulations indicate that the idea of nucleation of magnetisation reversal due to a rather wide distribution of anisotropy might be considered. Due to the resemblance in shape of hysteresis loops and SPHs with mostly reasonable parameters it seems that a micromagnetic model is suitable to describe and (in the near future) predict magnetisation processes in thin film media like Co-Cr for PMR.

With MFM we have studied written bits in a Co-Cr-Ta/NiFe layer up to recording densities of 300 kfrpi (89 nm bit length). Since the bits are smaller than the intrinsic domain structures (150 nm) here the bit shape is strongly influenced by relaxation processes in the decreasing field of the magnetic write head. These processes will determine the maximum reachable writing densities on these materials and are strongly determined by the micromagnetics of the switching process.

Summarising, the behaviour of Co-Cr down to a scale of 1  $\mu\text{m}$  can be understood from mean field theory. Below this scale, the steps of various size in Hall measurements show that discreet behaviour is present due microstructural properties like grain sizes and exchange inhomogeneity. Micromagnetic simulations show that we are beginning to understand what is happening on the sub-micron scale. The MFM results show that Co-Cr-Ta thin film is suitable for 100-200 kfrpi recording. For higher bit densities media with smaller intrinsic domain sizes are to be designed.

#### ACKNOWLEDGEMENT

The authors would like to thank J.N. Chapman, S. McVitie and D. Donnet of the University of Glasgow (UK) for supporting the Lorentz and DPC measurements. We would like to thank H. Muraoka and Y. Nakamura from the Tohoku University for cooperation and providing the

high density disks. This research has been partly financially supported by CAMST, a programme of the European Union.

#### REFERENCES

- [1] Y. Nakamura and H. Muraoka accepted paper DC-12, 6th joint MMM-Intermag, June 1994, Albuquerque, USA.
- [2] J.C. Lodder and T. Wielinga, IEEE Trans. Magn. MAG-20, 57 (1984).
- [3] J.G.Th. te Lintelo, J.C. Lodder, Th.J.A. Popma and J. Engemann, J. Magn.Magn.Mat, 115, 333 (1992)
- [4] J.G.Th. te Lintelo, W. Streekstra, J.C. Lodder and Th.J.A. Popma, IEEE Trans. Magn. MAG-29, 3748 (1993)
- [5] S. Chikazumi, 'Physics of magnetism', § 2.2, pp 19-24, John Wiley & Sons Inc., New York, (1964).
- [6] R. Street and J.C. Wooley, 'Proc. R. Phys. Soc. A 62, 562 (1949).
- [7] R. Street, R.K. Day and J.B. Dunlop, J. Magn. Magn. Mat. 69, 106 (1987).
- [8] J.G.Th. te Lintelo, J.C. Lodder, S. McVitie and J.N. Chapman, J. Appl. Phys. 75, 3002 (1994)
- [9] S. de Haan et al, to be published
- [10] M. van Kooten, S. de Haan, J.C. Lodder, Th.J.A. Popma, J. Appl. Phys. 75 (10), 5508 (1994)
- [11] S. de Haan, J.C. Lodder and Th.J.A. Popma, J. Magn. Soc. Jap. 15 Sup. S2,349 (1991)
- [12] B.C. Webb and S. Schultz, IEEE Trans. Magn. 24, 3006(1988)
- [13] Y. Maeda and M. Asahi, J. Appl. Phys. 61, 1972(1987)
- [14] J.C. Lodder, T. Wielinga and J. Worst, Thin Solid Films 101,61 (1982)
- [15] L. Néel, Adv. Phys. 4,191 (1955)
- [16] A.M. de Witte, K. O'Grady, G.N. Coverdale and R.W. Chantrell, J. Magn. Magn. Mat. 88,183 (1990)
- [17] M. van Kooten, S. de Haan, J.C. Lodder, A. Lyberatos, R.W. Chantrell and J.J. Miles, J. Magn. Magn. Mat. 120,145 (1993)
- [18] W.F. Brown Jr., Rev. Mod. Phys. 17,15 (1945)
- [19] M. van Kooten et al, to be published.
- [20] S. Porthun, M. Rührig and J.C. Lodder, acc. for publ. in: 'Forces in Scanning Probe Methods.' Eds.: H.J. Güntherodt, D. Anselmetti and E. Meyer. Kluwer Academic Publishers (1994).
- [21] M. Rührig, S. Porthun and J.C. Lodder, submitted to Rev. Sci. Instr. (1994).
- [22] H. Muraoka, Y. Nakamura, J. Mag. Soc. Jpn. 17, S2, 222 (in Japanese), (1993)